e-ISSN 2371-770X

Modern Medical Laboratory Journal

DOI: 10.30699/mmlj17.6.1.34

A deep learning-based technique for identifying COVID-19 from chest X-ray images

Ziba Bouchani[1*]

1. Department of Electrical and Computer Engineering, University of Tehran, Tehran, Iran.

KEYWORDS

COVID-19;

Support Vector Machine;

AlexNet;

Convolutional Neural Networks;

Lung Segmentation

Article Info

Received 2023/04/20;

Accepted 2023/05/17;

Published Online 2023

ABSTRACT

This study uses deep learning algorithms and CT (Computed Tomography) scans to diagnose COVID-19. First, we introduce a novel method to reduce noise in CT images by combining wavelet transformation with fuzzy logic. Then, using the suggested combined global and local threshold technique, we segmented lung pictures. Lung areas from CT scans can be successfully segregated in this manner. Features and categorization will be extracted in the following stage. While an SVM (Support Vector Machine) is used for classification, AlexNet extracts features. Three categories of data are categorized with a 99.8% accuracy: COVID-19, Viral Pneumonia, and Normal. The proposed strategy outperforms earlier approaches in terms of classification performance.

Corresponding Information: *Ziba Bouchani, Department of Electrical and Computer Engineering, University of Tehran, Tehran, Iran.*
Email: ziba.boochani1994@ut.ac.ir

Abbreviations

SVM, Support Vector Machine; ML, Machine Learning; DL, Deep Learning; MRI, Magnetic Resonance Imaging; CT, Computed Tomography; FMRI, Functional Magnetic Resonance Imaging; CNN, Convolutional Neural Network; WHO, World Health Organization

Introduction

Computer-aided detection and diagnosis performed using machine learning algorithms can help physicians interpret medical imaging findings and reduce interpretation times (1). Machine learning (ML) and deep learning (DL) applications that get the most of medical images, automating different steps of the clinical practice or providing support for clinical decisions. Disease diagnosis, image segmentation or outcome prediction are some of the tasks that are experiencing a disruptive transformation thanks to the latest progress of machine learning (2). As mentioned in (1), these algorithms have been used for several challenging tasks, such as brain tumor segmentation with magnetic resonance imaging (MRI) (3), pulmonary embolism segmentation with computed tomographic (CT) angiography (4), breast cancer detection and diagnosis with mammography (5), and detection of the cognitive state of the brain with fMRI (functional MRI) to diagnose neurologic disease like Alzheimer disease (6), and polyp detection with virtual colonoscopy or CT in the setting of colon cancer (7).

Due to strong transmission power of COVID-19, it has been spread quickly over the rest of the world after being discovered for the first time in Wuhan in 2019 (8). In 2020, the WHO (World Health Organization) classified it as a contagious, international illness (9). The presence of a temperature higher than 37.5 degrees Celsius, a dry cough, headaches, cramps, a loss of taste or smell, exhaustion, stomach symptoms, shortness of breath, and sore throats are all signs of this illness (10, 11). It shares symptoms with influenza, but there are more lung lesions (12). This illness results in death by inflaming the lungs and blocking the air sacs with secretions, which stops the body from receiving enough oxygen (13). The patient's recovery depends on a prompt and correct diagnosis of COVID-19 made early in the disease's progression (10). Additionally, it should be mentioned that prompt diagnosis of COVID-19 may result in the decision to hospitalize or confine the patient, reducing the risk of the virus spreading to others. Making a prompt and informed decision on whether to admit or discharge patients will tackle the issue of scarce healthcare resources, particularly hospital beds (9). According to reports, this test has a 30% false negative rate (14, 15). Its precision cannot be established as a result (14).

In rare circumstances, COVID-19 might be present, but the test won't find it. If the outcomes of these tests are negative, a computed tomography (CT) scan of the lungs may be necessary (15). With the aid of this lung imaging technology, patients can be evaluated quickly. Less than 20 minutes are needed to finish the process (10). To make diagnoses rapidly and without human mistake, deep learning approaches are being used to analyse medical images nowadays (12, 13, 16-18). According to a 2020 review study by Albahri et al., machine learning algorithms are particularly helpful in lowering the prevalence of the COVID-19 disease and its negative effects by offering quick, accurate, and affordable diagnostic and prediction models (19). Feature extraction occurs through the first layers of a convolutional neural network (CNN) architecture, and classification occurs in the final layers. The design of architecture is critical to the success of classification and the extraction of features. In the past ten years, a number of pre-trained and pre-designed CNN architectures, such as AlexNet (20), GoogLeNet (21), ResNet (22), VGG-Net (23), DenseNet (24), and Inceptionv3 (25), have been developed. These designs have produced satisfactory results in image classification and pattern identification. Various DL and transfer learning-based researches have employed this pre-trained CNN model. Pre-trained CNN architectures were utilized by Ardakani et al. (26) to separate COVID-19 cases from non-COVID cases using CT scans. Each model of a convolutional neural network has benefits and drawbacks. For instance, the AlexNet classifier is more accurate than the others but takes longer to produce more accurate results due to the low depth (27). Although VGG (23) has a deeper depth than AlexNet, gradients vanish as the deeper depth of VGG is increased. A GoogleNet (28) training program has a higher computational complexity than a VGG training method but is faster. Compared to GoogleNet, MobileNet (29) has fewer computations and parameters, and it has a low latency. Its precision is a little poorer, though. The issue of vanishing gradients has been resolved by ResNet (30). Additionally, it takes less time to train. But it has a convoluted architectural design.

Proposed Method and Results

Three classes of people will be distinguished in this article: COVID-19 (people suffering from COVID-19), Normal (healthy people), and Viral (people caught a cold). For this purpose, we use CT scan images of the lungs available in (31-33). Figure 1 depicts our suggested approach, and Table 1 lists the number of samples for each class.

Figure 1. The block diagram of the proposed method.

Table 1. Numbers of classes in the COVID-19 Database

Class of People	Covid-19	Normal	Viral
Number of Samples	219	1341	1345

In the following, the details of the algorithm's steps will be explained.

Noise Reduction

Images frequently contain noise due to transmission issues or sensor errors. The effectiveness of future image processing procedures segmentation, object detection, etc. is decreased by image noise. In order to speed up imaging and reduce the quantity of X-ray radiation that the patient is exposed to, it is crucial to employ an appropriate filter to reduce noise in medical images. This scenario can improve a doctor's comprehension of the captured image, hence reducing medical errors. To eliminate noise, we threshold wavelet coefficients, where the threshold value is applied consistently across all picture values. In addition, we apply fuzzy logic to avoid visual distortion, enabling highly precise denoising. As a result, the suggested method offers a fresh strategy for eliminating noise and addressing the issues in this field by combining fuzzy logic and wavelet processing.

Semantic Lung segmentation

In this part, we presented a novel technique for separating the lung from other tissues based on region-based segmentation. For this, the global threshold is initially employed. With global thresholds, the threshold value is regarded as constant throughout the entire image. For a gray picture I (x, y), a binary image g (x, y) is produced by global thresholding T:

$$g(x,y) = \begin{cases} 0 & if\ intensity\ at\ point\ (x,y) < T \\ 1 & otherwise \end{cases}$$

Threshold T can be calculated in a variety of ways, but histogram-based techniques are the most popular. If an item and backdrop both have the same brightness, the histogram of the image will have two peaks, as seen in Figure 2. In this case, the threshold value is determined by the local minimum between the histogram's two peaks.

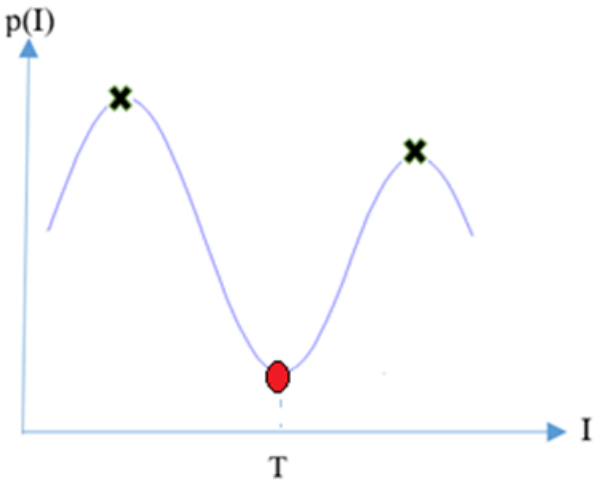

Figure 2. In the histogram of a two-dimensional gray image, the minimum value between two peaks is selected as threshold value in thresholding method

Getting the histogram of the region of interest, which is close to the center of the image, is the first step in the suggested algorithm. The range of gray levels used in the iterative thresholding method is defined by this histogram. The algorithm should be run seven times with each iteration increasing the threshold within a predetermined range of gray levels. Constructing contours around a group of adjacent bright pixels requires an eight-point connection map.

At the center of mass of each contour, a profile is created to see if it comprises lung pixels. The binary picture produced is used to extract pixels from the contour that was found to be outside the lung during future iterations.

The seventh iteration brings us to the solution set of initial contours. To totally isolate the lung during the initial contouring process, we employ the local thresholding technique. By thresholding a few local pixels around the area of interest, a composite binary picture is created to produce the final contour set. The rolling ball (34) algorithm is used to remove substantial disturbances and inhomogeneities from the contour after it has been smoothed. The angles are then established, and the precise segmentation of the lung is established. With horizontal and vertical shiny lines, the computer indicates the middle part of the lung and the external boundary of the lung. In Figure 3, this procedure is displayed.

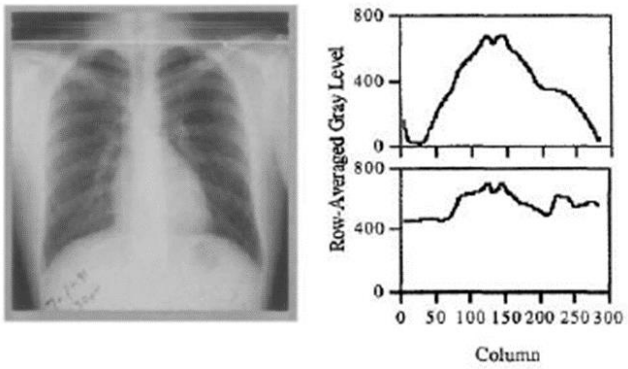

Figure 3. The computer marks the middle part of the lung and the external boundary of the lung with horizontal and vertical shiny lines.

The Sobel filter (35) is twisted with 1/4 on the bottom and right side of the image to highlight aperture lines and faint edges. Large contours cannot be formed because it is attached to the intestine. By using the histogram to distinguish between the gray levels that belong to pixels inside the lung and those that belong to pixels outside the lung, global thresholding is utilized to determine the appropriate gray level. The contours around the lung will be too narrow and insufficient if the gray level is too low. The lung area will follow the same contour as the surrounding area if the gray levels are too high. Therefore, finding the appropriate threshold with only one gray level is impossible. Iterative global thresholding, which uses a range rather than a single value, can be utilized to solve this issue.

As shown in Figure 4, the slope of the global histogram is utilized to identify the gray levels that represent lung events. The range of gray levels between these two places is then used to guide the application of a global thresholding approach. Seven sites in this range with similar distances are successively thresholded as part of an iterative procedure. In the first iteration of the method, a binary picture is produced using the lowest gray level among the seven possible levels as a threshold. Bright pixels in a binary image are those that have gray levels below the threshold. In this way, a contour is created around the binary image obtained and gradually improves over time. It is possible to determine the contour's center, degree of compression, length, and area, among other geometrical characteristics. Two binary pictures with various thresholds from the original image are obtained in Figure 5. In sub-figure A, the threshold is lower than in sub-figure B.

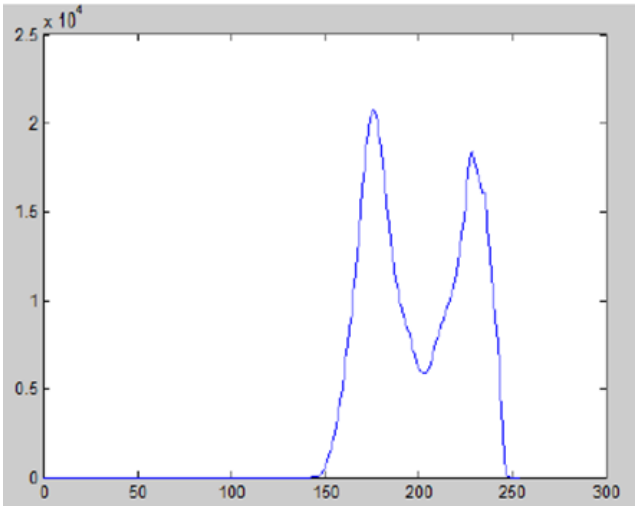

Figure 4. During the subsequent iterations, the thresholds are also increased, creating additional binary images. A global histogram shows a bimodal distribution. Arrows indicate which pixels belong to the lung and intermediate frames.

Figure 5. Obtaining two binary images with different thresholds from the original image. The threshold used in sub-figure A is lower than that used in sub-figure B.

After every three repetitions, the binary picture is opened using the 33 kernels of the morphological operator (36). As seen in Figure 6, the opening operator removes a number of image artifacts (the erosion operator followed by the dilation operator), so we have well-done lung image segmentations.

Figure 6. An example of well-done lung image segmentation by the proposed method.

Data Augmentation

To produce precise predictions using the deep learning and machine learning approach, a sizable dataset is required. There is a problem with the availability of large quantities of data in many fields. Computers are therefore utilized in numerous applications to enhance data and provide reliable classifications. This application employs a rotation technique between -25 and +25, as well as a 10% shift in both the horizontal and vertical axes, as depicted in Figure 7. Therefore, Images of the COVID-19 class scans with fewer samples than others have been rotated or shifted (see Table 1). The data augmentation has resulted in 1225 samples being added to the COVID-19 class.

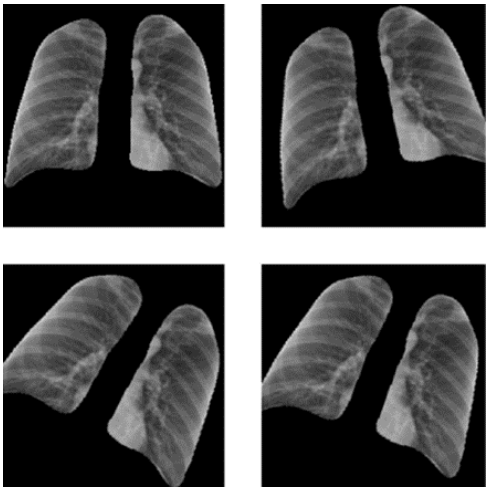

Figure 7. An example of rotation and shift technique for data augmentation in one lung image.

Classification via CNN+SVM model

The data is sent into deep CNN after the elimination of noise from the lung images during the pre-processing stage and the separation of lungs using the suggested thresholding method. The CNN model is considered as an AlexNet architecture for feature extraction in this article, and the picture size has been modified to 227×227×3. We employ SVM to increase classification accuracy. We can attain a classification accuracy of 99.8% with this method. Figure 8 depicts the block diagram of the suggested strategy for classifying CT scans into three categories: COVID-19 (people suffering from COVID-19), Normal (healthy people), and Viral (people caught a cold). To examine the results of the categorization, we employed the accuracy, recall, and specificity metrics. Accuracy shows how often a classification model is correct overall. Recall illustrates whether a model can find all objects of the target class, and specificity depicts the ability of a test to correctly classify an individual as a disease. Equations (1) to (3) introduce these measurements:

$$Accuracy = \frac{tp + tn}{tp + fp + tn + fn} x100 \quad (1)$$

$$Recall = \frac{tp}{tp + fn} \quad (2)$$

$$Specificity = \frac{tn}{tn + fp} \quad (3)$$

Where tp is true positive; tn is true negative; fp is false positive; and finally fn is false negative.

As a result, 0.9983, 0.9991, and 0.9983 are the findings for Accuracy, Recall, and Specificity, respectively. The outcomes clearly show how accurate the suggested strategy is. The preprocessing and input of segmented lung images to the CNN model is the main distinction and superiority of the suggestion technique. Figure 9 displays the outcomes of the suggested CNN + SVM structure's successful classification of the input images. As it can easily be seen, in sub-figure A, the lung is really damaged and our system has accurately classified this image as COVID. For sub-figure B, the lung is a little damaged which is not because of COVID, and is related to a mild viral e.g. a cold as our method correctly distinguished this fact. Finally, in sub-figure C, the lung is totally healthy and the image is assigned to the Normal class.

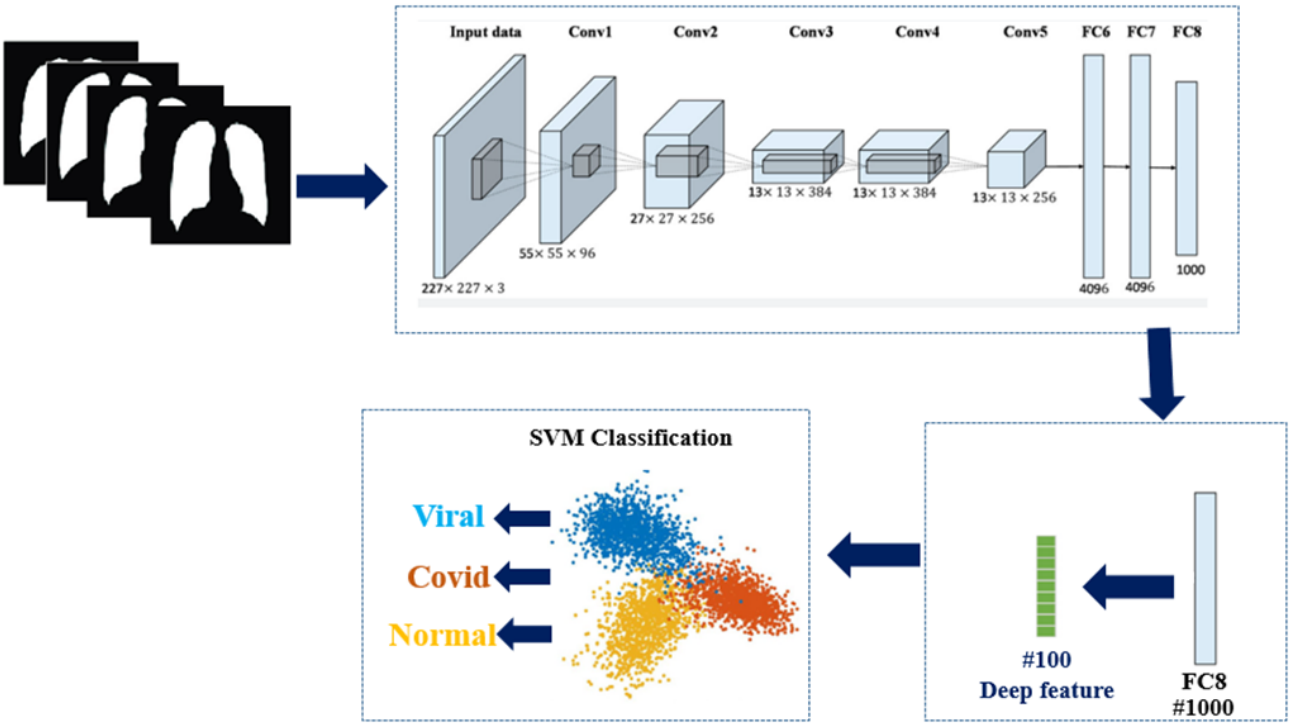

Figure 8. The block diagram of the proposed method of classifying CT images into three classes i.e. viral, COVID, and normal. Firstly, lung images are entered into the AlexNet architecture for feature extraction, and then by using SVM for more accurate classification, being viral, COVID, or normal of each image is determined precisely and automatically.

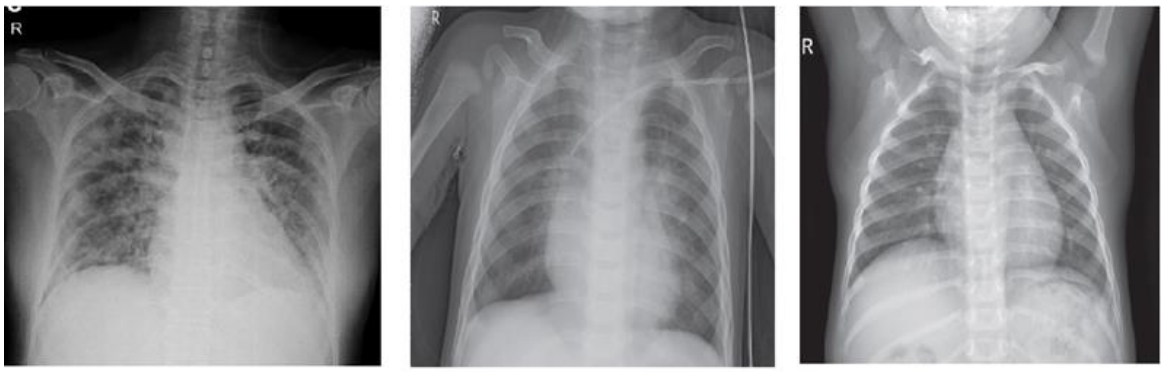

Figure 9. An example of lung image classification, A: COVID-19 lung image, B: Viral lung image, and C: Normal lung image.

Conclusion

Early detection is crucial if we want to stop the COVID-19 epidemic from spreading. A difference between this study and others is that it begins by semantically segmenting the CT images and then applies those segments to deep learning algorithms. Lung CT images are segmented using semantic segmentation. Three-class CT images can be distinguished with 99.8% accuracy using the proposed AlexNet + SVM network. The success of the investigation depends on the segmentation of the lungs. Features have been retrieved from raw photos in earlier studies.

This study has been proven to perform better than earlier ones of its kind. Without using any custom feature extraction techniques, the suggested program automatically classifies lung pictures for COVID-19 diagnosis after semantic segmentation. When the prediction is made using solely lung images, the feature extraction algorithm produces more accurate features. This is so because the characteristics are taken from the region where the disease is most prevalent. This technique was created as a quick, reliable decision assistance system that can help highly qualified radiologists. As a result, radiologists may handle less work, avoid incorrect diagnoses, and spot illnesses before they spread.

Declaration

Funding
Not available.

Conflicts of interest/Competing interests
The author declares no conflict of interest.

Authors' contributions
ZB designed the study concept, collected and interpreted the data and drafted the manuscript.

Ethics approval
Not applicable.

References

1. Erickson BJ, Korfiatis P, Akkus Z, Kline TL. Machine learning for medical imaging. Radiographics. 2017;37(2):505-15.

2. Barragán-Montero A, Javaid U, Valdés G, Nguyen D, Desbordes P, Macq B, et al. Artificial intelligence and machine learning for medical imaging: A technology review. Physica Medica. 2021;83:242-56.

3. Bauer S, Wiest R, Nolte L-P, Reyes M. A survey of MRI-based medical image analysis for brain tumor studies. Physics in Medicine & Biology. 2013;58(13):R97.

4. Pu J, Gezer NS, Ren S, Alpaydin AO, Avci ER, Risbano MG, et al. Automated detection and segmentation of pulmonary embolisms on computed tomography pulmonary angiography (CTPA) using deep learning but without manual outlining. Medical Image Analysis. 2023;89:102882.

5. Al-Tam RM, Narangale SM. Breast cancer detection and diagnosis using machine learning: a survey. J Sci Res. 2021;65(5):265-85.

6. Sarraf S, Tofighi G. Classification of alzheimer's disease using fmri data and deep learning convolutional neural networks. arXiv preprint arXiv:160308631. 2016.

7. Grosu S, Wesp P, Graser A, Maurus S, Schulz C, Knösel T, et al. Machine learning–based differentiation of benign and premalignant colorectal polyps detected with CT Colonography in an asymptomatic screening population: a proof-of-concept study. Radiology. 2021;299(2):326-35.

8. Secco G, Delorenzo M, Salinaro F, Zattera C, Barcella B, Resta F, et al. Lung ultrasound presentation of COVID-19 patients: phenotypes and correlations. Internal and Emergency Medicine. 2021;16:1317-27.

9. Buda N, Segura-Grau E, Cylwik J, Wełnicki M. Lung ultrasound in the diagnosis of COVID-19 infection-A case series and review of the literature. Advances in medical sciences. 2020;65(2):378-85.

10. Sultan LR, Sehgal CM. A review of early experience in lung ultrasound in the diagnosis and management of COVID-19. Ultrasound in Medicine & Biology. 2020;46(9):2530-45.

11. Volpicelli G, Gargani L, Perlini S, Spinelli S, Barbieri G, Lanotte A, et al. Lung ultrasound for the early diagnosis of COVID-19 pneumonia: an international multicenter study. Intensive care medicine. 2021;47:444-54.

12. Rajpal S, Lakhyani N, Singh AK, Kohli R, Kumar N. Using handpicked features in conjunction with ResNet-50 for improved detection of COVID-19 from chest X-ray images. Chaos, Solitons & Fractals. 2021;145:110749.

13. Ahsan M, Based MA, Haider J, Kowalski M. COVID-19 detection from chest X-ray images using feature fusion and deep learning. Sensors. 2021;21(4):1480.

14. Sorlini C, Femia M, Nattino G, Bellone P, Gesu E, Francione P, et al. The role of lung ultrasound as a frontline diagnostic tool in the era of COVID-19 outbreak. Internal and emergency medicine. 2021;16:749-56.

15. Colombi D, Petrini M, Maffi G, Villani GD, Bodini FC, Morelli N, et al. Comparison of admission chest computed tomography and lung ultrasound performance for diagnosis of COVID-19 pneumonia in populations with different disease prevalence. European journal of radiology. 2020;133:109344.

16. Horry MJ, Chakraborty S, Paul M, Ulhaq A, Pradhan B, Saha M, et al. COVID-19 detection through transfer learning using multimodal imaging data. Ieee Access. 2020;8:149808-24.

17. Born J, Brändle G, Cossio M, Disdier M, Goulet J, Roulin J, et al. POCOVID-Net: automatic detection of COVID-19 from a new lung ultrasound imaging dataset (POCUS). arXiv preprint arXiv:200412084. 2020.

18. Roy S, Menapace W, Oei S, Luijten B, Fini E, Saltori C, et al. Deep learning for classification and localization of COVID-19 markers in point-of-care lung ultrasound. IEEE transactions on medical imaging. 2020;39(8):2676-87.

19. Albahri AS, Hamid RA, Alwan JK, Al-Qays Z, Zaidan A, Zaidan B, et al. Role of biological data mining and machine learning techniques in detecting and diagnosing the novel coronavirus (COVID-19): a systematic review. Journal of medical systems. 2020;44:1-11.

20. Han J, Zhang D, Cheng G, Liu N, Xu D. Advanced deep-learning techniques for salient and category-specific object detection: a survey. IEEE Signal Processing Magazine. 2018;35(1):84-100.

21. Al-Dhamari A, Sudirman R, Mahmood NH. Transfer deep learning along with binary support vector machine for abnormal behavior detection. IEEE Access. 2020;8:61085-95.

22. Yu S, Xie L, Liu L, Xia D. Learning long-term temporal features with deep neural networks for human action recognition. IEEE Access. 2019;8:1840-50.

23. Simonyan K, Zisserman A. Very deep convolutional networks for large-scale image recognition. arXiv preprint arXiv:14091556. 2014.

24. Huang G, Liu Z, Van Der Maaten L, Weinberger KQ, editors. Densely connected convolutional networks. Proceedings of the IEEE conference on computer vision and pattern recognition; 2017.

25. Szegedy C, Vanhoucke V, Ioffe S, Shlens J, Wojna Z, editors. Rethinking the inception architecture for computer vision. Proceedings of the IEEE conference on computer vision and pattern recognition; 2016.

26. Ardakani AA, Kanafi AR, Acharya UR, Khadem N, Mohammadi A. Application of deep learning technique to manage COVID-19 in routine clinical practice using CT images: Results of 10 convolutional neural networks. Computers in biology and medicine. 2020;121:103795.

27. Krizhevsky A, Sutskever I, Hinton GE. ImageNet classification with deep convolutional neural networks. Communications of the ACM. 2017;60(6):84-90.

28. Szegedy C, Liu W, Jia Y, Sermanet P, Reed S, Anguelov D, et al., editors. Going deeper with convolutions. Proceedings of the IEEE conference on computer vision and pattern recognition; 2015.

29. Howard AG, Zhu M, Chen B, Kalenichenko D, Wang W, Weyand T, et al. Mobilenets: Efficient convolutional neural networks for mobile vision applications. arXiv preprint arXiv:170404861. 2017.

30. He K, Zhang X, Ren S, Sun J, editors. Deep residual learning for image recognition. Proceedings of the IEEE conference on computer vision and pattern recognition; 2016.

31. Cohen JP, Morrison P, Dao L, Roth K, Duong TQ, Ghassemi M. Covid-19 image data collection: Prospective predictions are the future. arXiv preprint arXiv:200611988. 2020.

32. Kermany D, Zhang K, Goldbaum M. Labeled optical coherence tomography (oct) and chest x-ray images for classification. Mendeley data. 2018;2(2).

33. COVID A. Chest X-ray Dataset. 2020.

34. Pater Z, Tomczak J, Wójcik Ł, Bulzak T. Physical modelling of the ball-rolling processes. Metals. 2019;9(1):35.

35. Gao W, Zhang X, Yang L, Liu H, editors. An improved Sobel edge detection. 2010 3rd International conference on computer science and information technology; 2010: IEEE.

36. Kermany D, Zhang K, Goldbaum M. Labeled optical coherence tomography (oct) and chest x-ray images for classification. Mendeley data. 2018;2(2):651.

How to cite this article: Bouchani Z. A deep learning-based technique for identifying COVID-19 from chest X-ray images. Mod Med Lab J. 2023;6(1): 34-41.